SUPPLEMENTARY DATA

for

PHASE TRANSFORMATIONS IN THE Fe-AsO_4-SO_4 SYSTEM AND STRUCTURE OF AMORPHOUS FERRIC ARSENATE: IMPLICATIONS FOR ARSENIC STABILIZATION IN MINE DRAINAGE AND INDUSTRIAL EFFLUENTS

DOGAN PAKTUNC

CANMET, Natural Resources Canada, 555 Booth St., Ottawa, ON, K1A 0G1 Canada

Transmission Electron Microscopy Characterization

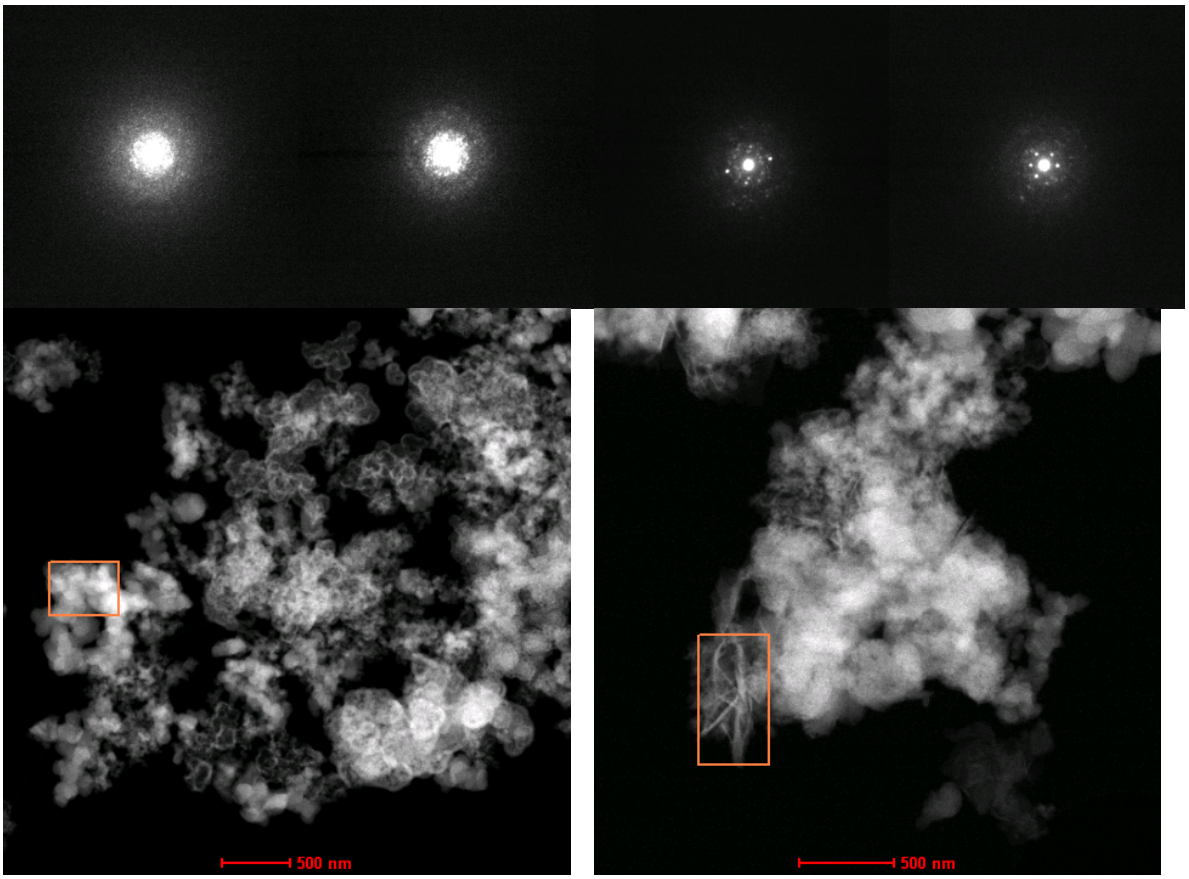

Figure S1. Nano-probe diffraction using a beam diameter of a few nanometers obtained from ferric arsenate (left) and scorodite (right). Probe locations are marked on scanning transmission electron microscopy (STEM) images below.

Reassessment of framework model

In their response to the comment by Paktunc and Manceau (2013), Mikutta et al. (2013) maintained their view on the local structure of ferric arsenate by providing new fits with different fit parameters and a revised fit strategy. The changes to the fit strategy are significant which included (1) addition of the Fe-As-O MS path with its Debye-Waller parameter (σ^2) fixed to 0.007 Å^2, (2) floating the $CN_{Fe\text{-}As}$ path, (3) scaling $CN_{Fe\text{-}O2}$, $CN_{Fe\text{-}O3}$ and $CN_{Fe\text{-}O4}$ to $CN_{Fe\text{-}As}$, (4) fixing $\sigma^2_{Fe\text{-}O2} = \sigma^2_{Fe\text{-}O3} = \sigma^2_{Fe\text{-}O4} = \sigma^2_{Fe\text{-}O1}$ and (5) fixing $\sigma^2_{Fe\text{-}O\text{-}O(T)} = \sigma^2_{Fe\text{-}O\text{-}O(C)} = \sigma^2_{Fe\text{-}O\text{-}Fe\text{-}O} = 2\times\sigma^2_{Fe\text{-}O1}$. The fit results reported by Mikutta

et al. (2013) were reproduced only when $\sigma^2_{Fe\text{-}As\text{-}O}$ is fixed to 0.007 Å^2 as in Mikutta et al. (2013). Our fit results are comparable with the exception of $CN_{Fe\text{-}As}$, $CN_{Fe\text{-}O2}$, $CN_{Fe\text{-}O3}$ and $CN_{Fe\text{-}O4}$. Inclusion of the Fe-As-O path helped to better simulate the 2nd Fourier-transform peak and the fit quality is improved over the authors' original fit results (Table 2 in manuscript). However, the problems with the fit strategy still exist. First of all, a justification is not provided for fixing $\sigma^2_{Fe\text{-}As\text{-}O}$ to 0.007 Å^2, which represents the upper value of the As-Fe-O path (i.e. 0.005±0.002 Å^2). Secondly, this value is lower than $\sigma^2_{Fe\text{-}As}$ (i.e. preceding SS Fe-As path); therefore, it is unrealistic because MS contributions have higher effective disorders than their corresponding SS contributions as pointed out by Paktunc and Manceau (2013). Thirdly, the fixed value of 8 for the CN of the Fe-As-O path does not make sense for a floating $CN_{Fe\text{-}As}$ because it produces unphysical values for cases when $CN_{Fe\text{-}As}$ is less than 4. Instead, $CN_{Fe\text{-}As\text{-}O}$ should have been scaled to $2\times CN_{Fe\text{-}As}$. More reasonable approaches such as using a fixed $\sigma^2_{As\text{-}Fe\text{-}O}$ from the corresponding As-EXAFS fit or floating $\sigma^2_{Fe\text{-}As\text{-}O}$ produced strong correlations and resulted in unrealistic radial distances (i.e. $R_{Fe\text{-}O3} = R_{Fe\text{-}O4} = 3.91\pm 60.00$ Å).

Mikutta et al. (2014) revised their EXAFS fit strategy and parameters once again; however, the earlier inconsistencies in their fit strategies remain. Shell fit parameters for the Fe K-edge EXAFS of an analogous amorphous ferric phosphate included scaling of CNs of O2, O3, O4 to CN of O1 to artificially increase the amplitude of the distant O paths for an improved fit. This strategy has no physical sense because the CNs of the distant O paths extending to PO_4 tetrahedra and the Fe-O paths within the octahedra are totally unrelated.

Table S1. Local structural parameters of ferric arsenate precipitates determined from simultaneous fitting of Fe K-edge and As K-edge EXAFS spectra

path	CN	*R*	σ^2	path	N	*R*	σ^2
F3-66	*($E0_{Fe}$=-2.1; $E0_{As}$=6.1; rf=0.010)*						
Fe-O	5.7±0.4	1.99±0.01	0.0077	As-O	4.4±0.3	1.69±0.00	0.0028
Fe-As	2.1±1.0	3.32±0.01	0.0089	As-Fe	2.3±0.9	3.32	0.0089
Fe-Fe	2	3.58±0.02	0.0118				
Fe-O-O (T)	24	3.57±0.16	0.0154	As-O-O	12	3.13±0.06	0.0056
Fe-O-O (C)	6	4.02±0.12	"				

F3-114	*($E0_{Fe}$=-1.6; $E0_{As}$=5.3; rf=0.009)*						
Fe-O	5.6±0.4	1.99±0.00	0.0077	As-O	4.2±0.3	1.69±0.00	0.0024
Fe-As	2.4±1.2	3.32±0.01	0.0095	As-Fe	2.4±0.9	3.32	0.0095
Fe-Fe	2	3.59±0.02	0.0121				
Fe-O-O (T)	24	3.52±0.16	0.0154	As-O-O	12	3.12±0.05	0.0048
Fe-O-O (C)	6	4.05±0.14	"				
F1-18	*($E0_{Fe}$=-1.3; $E0_{As}$=5.3; rf=0.010)*						
Fe-O	5.5±0.5	1.99±0.01	0.0076	As-O	4.2±0.3	1.69±0.00	0.0024
Fe-As	2.5±1.5	3.32±0.01	0.0093	As-Fe	2.3±1.0	3.32	0.0093
Fe-Fe	2	3.59±0.03	0.0134				
Fe-O-O (T)	24	3.52±0.20	0.0152	MS1	12	3.12±0.05	0.0048
Fe-O-O (C)	6	4.07±0.18	"				
FS-1	*($E0_{Fe}$=-1.9; $E0_{As}$=5.3; rf=0.012)*						
Fe-O	5.8±0.3	1.99±0.00	0.0083	As-O	4.5±0.4	1.69±0.00	0.0028
Fe-As	1.8±1.1	3.32±0.01	0.0088	As-Fe	2.5±1.1	3.32	0.0088
Fe-Fe	2	3.58±0.03	0.0146				
Fe-O-O (T)	24	3.47±0.11	0.0166	As-O-O	12	3.13±0.08	0.0057
Fe-O-O (C)	6	4.08±0.10	"				
F2-120	*($E0_{Fe}$=-1.8; $E0_{As}$=5.1; rf=0.012)*						
Fe-O	5.8±0.4	1.99±0.00	0.0079	As-O	4.1±0.4	1.69±0.00	0.0023
Fe-As	2.6±1.4	3.32±0.01	0.0098	As-Fe	2.7±1.2	3.32	0.0098
Fe-Fe	2	3.58±0.02	0.0110				
Fe-O-O (T)	24	3.54±0.15	0.0158	As-O-O	12	3.13±0.07	0.0045
Fe-O-O (C)	6	4.02±0.12	"				
F6-239	*($E0_{Fe}$=-1.5; $E0_{As}$=5.1; rf=0.011)*						
Fe-O	5.8±0.3	1.99±0.00	0.0081	As-O	4.3±0.3	1.69±0.00	0.0025
Fe-As	1.7±0.9	3.31±0.01	0.0080	As-Fe	2.4±0.9	3.31	0.0080
Fe-Fe	2	3.57±0.03	0.0156				
Fe-O-O (T)	24	3.47±0.10	0.0162	As-O-O	12	3.14±0.07	0.0051
Fe-O-O (C)	6	4.09±0.09	"				
F7-119	*($E0_{Fe}$=-1.7; $E0_{As}$=5.3; rf=0.010)*						
Fe-O	5.5±0.3	1.99±0.00	0.0074	As-O	4.2±0.3	1.69±0.00	0.0024
Fe-As	2.4±1.3	3.32±0.01	0.0099	As-Fe	2.5±1.0	3.32	0.0099
Fe-Fe	2	3.59±0.02	0.0116				
Fe-O-O (T)	24	3.5±0.12	0.0148	As-O-O	12	3.12±0.06	0.0048
Fe-O-O (C)	6	4.06±0.11	"				
B14-2	*($E0_{Fe}$=-2.2; $E0_{As}$=3.6; rf=0.010)*						
Fe-O	5.7±0.4	1.99±0.00	0.0078	As-O	3.6±1.2	1.68±0.00	0.0027
Fe-As	2.7±1.4	3.32±0.01	0.0088	As-Fe	2.3±0.8	3.32	0.0088
Fe-Fe	2	3.57±0.03	0.0133				
Fe-O-O (T)	24	3.45±0.11	0.0157	As-O-O	12	3.10±0.06	0.0054
Fe-O-O (C)	6	4.07±0.10					

B12-23	*($E0_{Fe}$=-1.9; $E0_{As}$=4.4; rf=0.010)*						
Fe-O	5.5±0.4	1.99±0.00	0.0080	As-O	4.3±0.3	1.69±0.00	0.0029
Fe-As	3.6±1.7	3.33±0.01	0.0098	As-Fe	2.2±0.9	3.33	0.0098
Fe-Fe	2	3.58±0.03	0.0094				
Fe-O-O (T)	24	3.52±0.15	0.0159	As-O-O	12	3.10±0.06	0.0057
Fe-O-O (C)	6	4.01±0.12					
B12-34	*($E0_{Fe}$=-1.5; $E0_{As}$=4.0; rf=0.016)*						
Fe-O	5.1±0.5	1.99±0.01	0.0076	As-O	4.6±0.3	1.69±0.00	0.0030
Fe-As	2.0±1.3	3.32±0.01	0.0078	As-Fe	2.0±0.8	3.32	0.0078
Fe-Fe	2	3.55±0.04	0.0148				
Fe-O-O (T)	24	3.44±0.13	0.0153	As-O-O	12	3.10±0.07	0.0060
Fe-O-O (C)	6	4.09±0.12					
B7-1	*($E0_{Fe}$=-1.8; $E0_{As}$=4.9; rf=0.009)*						
Fe-O	5.6±0.4	1.99±0.00	0.0078	As-O	4.0±0.3	1.69±0.00	0.0022
Fe-As	3.4±1.7	3.33±0.01	0.0102	As-Fe	2.3±0.9	3.33	0.0102
Fe-Fe	2	3.59±0.03	0.0106				
Fe-O-O (T)	24	3.55±0.16	0.0156	As-O-O	12	3.12±0.05	0.0044
Fe-O-O (C)	6	4.02±0.13	"				
B7-22	*($E0_{Fe}$=-1.4; $E0_{As}$=6.4; rf=0.017)*						
Fe-O	5.2±0.5	1.99±0.01	0.0077	As-O	4.4±0.3	1.69±0.00	0.0029
Fe-As	1.8±1.2	3.32±0.01	0.0074	As-Fe	2.0±0.9	3.32	0.0074
Fe-Fe	2	3.55±0.05	0.0172				
Fe-O-O (T)	24	3.44±0.13	0.0154	As-O-O	12	3.15±0.08	0.0059
Fe-O-O (C)	6	4.10±0.12	"				
B8-2	*($E0_{Fe}$=-2.0; $E0_{As}$=4.3; rf=0.013)*						
Fe-O	5.3±0.3	1.99±0.00	0.0077	As-O	4.5±0.4	1.69±0.00	0.0031
Fe-As	3.2±1.6	3.32±0.01	0.0103	As-Fe	2.7±1.1	3.32	0.0130
Fe-Fe	2	3.58±0.03	0.0122				
Fe-O-O (T)	24	3.48±0.10	0.0154	As-O-O	12	3.13±0.08	0.0061
Fe-O-O (C)	6	4.07±0.09	"				

CN: coordination number; *R*: interatomic distance (Å); σ^2: Debye–Waller parameter (Å^2); *E0*: energy offset (eV); *rf*: r-factor and rX^2 reduced chi square as the goodness-of-fit parameters; Fits performed in *R*-space with *R*=0.8-3.5 Å, *k*=3-15 Å^{-1} and amplitude reduction factor (S_0^2) constrained to 1.0 for As-EXAFS, and *R*=1-4 Å, *k*=2-14 Å^{-1} and amplitude reduction factor (S_0^2) constrained to 0.9 for Fe-EXAFS; Fe-O-O (T): triangular MS path ; Fe-O-O (C): collinear MS path; Refer to Table 3 for fit strategy.

References

MIKUTTA, C., MANDALIEV, P.N., & KRETZSCHMAR, R. (2013) Response to Comment on “New Clues to the Local Atomic Structure of Short-Range Ordered

Ferric Arsenate from Extended X‐ray Absorption Fine Structure Spectroscopy". Environmental Science and Technology, 47, 13201-13202.

MIKUTTA, C., SCHRODER, C., & MICHEL, F.M. (2014) Total X-ray scattering, EXAFS, and Mossbauer spectroscopy analyses of amorphous ferric arsenate and amorphous ferric phosphate. Geochimica et Cosmochimica Acta, 140, 708-719.

PAKTUNC, D. & MANCEAU, A. (2013) Comment on "New clues to the Local Atomic Structure of Short-Range Ordered Ferric Arsenate from Extended X-ray Absorption Fine Structure Spectroscopy". Environmental Science and Technology, 47, 13199-13200.